Description of rock types and main deformation features within the Kuiseb section

The measured section is exposed along the Kuiseb River on the farm Niedersachsen, 160 km west of Windhoek (23˚09.32' S; 15˚54.88' E). The Kuiseb Formation in this section comprises cm- to meter-thick metasandstones and metasiltstone, interlayered in turbiditic sequences with metapelite intervals, and volumetrically minor calcsilicate felses, scapolite schist and layers of marble (see also Kukla, 1992). Metasandstones are light- to dark-grey, generally massive and locally graded, dominated by granoblastic quartz and plagioclase. Interlayered kyanite-zone metapelites are micaschists with biotite and white mica as well as garnet and staurolite with or without kyanite and, in places, retrograde chlorite, indicating an amphibolite-grade, Barrovian-type metamorphism associated with subduction. The metamafic rocks of the Matchless Amphibolite Belt are represented in the traverse by very fine-grained metabasalt and medium- to coarse-grained metagabbro. Metabasalts are generally massive and composed of hornblende, plagioclase and epidote. The metagabbro comprises metamorphic amphibole and plagioclase and occurs exclusively in the structurally lower part of the section as meters to tens of meters thick lensoid-shaped bodies with locally well-preserved primary textures.
Deformation in the section is characterized by progressive folding, cleavage development and thrusting with the formation of intense, shear-dominated transposed and mylonitic fabrics. The most penetrative planar element in all rock types is a flat-lying composite foliation (Sp) defined by the preferential orientation of white mica and biotite, hornblende and staurolite as well as a mm-scale compositional layering in the psammitic sections. The orientation of Sp is very uniform and sub-parallel to bedding (Figs 2, 3), representing a composite foliation surface resulting from shear-related transposition of different planar fabrics developed during progressive deformation. The Sp plane contains a stretching lineation, Lp, generally oblique with respect to Sp dip direction, and defined by the alignment of quartz, biotite and plagioclase, and porphyroblasts of hornblende, staurolite, and kyanite, where present. Sp is axial planar to intrafolial, tight- to isoclinal, commonly asymmetric, SE-verging folds. Other kinematic indicators are S-C structures and, locally, S-C' structures with sense of elongation parallel to Lp lineation. All structures indicate a top to the SE sense of shear, consistent with the main structural vergence of the Southern Zone.

Analytical Methods

U/Pb zircon data were collected for Salem Granite samples N13 and N18 at the Centre for Analytical Facilities (CAF) LA-ICP-MS unit, Stellenbosch University, South Africa, using a 213 nm New Wave laser coupled with an Agillent 7500ce quadrupole ICP-MS. The analytical method follows that given in Lana et al. (2011). Briefly, zircons were separated from crushed and sieved rock by panning and magnetic separation. Hand-picked grains were mounted in epoxy disks that were ground down and then polished to expose grain centres. Zircon grains were imaged in cathodoluminescence (CL) mode using a LEO 1450VP SEM (Stellenbosch University). LA-ICP-MS operating conditions were optimised to provide maximum sensitivity for the high masses (Pb–U) while inhibiting oxide formation (ThO+/Th+<0.5%). Ablations occurred in a custom-built small-volume, teardrop-shaped sample cell (Horstwood et al., 2003) in a He carrier gas, and the resulting aerosol was mixed with Ar prior to introduction into the ICP-MS via a signal-

smoothing manifold ("squid"). Data reduction used the Glitter software package (van Achterbergh et al., 2001) to calculate the relevant isotopic ratios ($^{207}Pb/^{206}Pb$, $^{208}Pb/^{206}Pb$, $^{208}Pb/^{232}Th$, $^{206}Pb/^{238}U$ and $^{207}Pb/^{235}U$). ^{235}U was calculated from ^{238}U counts via the natural abundance ratio $^{235}U = {}^{238}U/137.88$ (Jackson et al., 2004). Individual isotopic ratios were displayed in time-resolved mode, and ablation depth-dependent elemental fractionation was corrected for by tying the integration window for the unknown to the identical integration window of the standard (Jackson et al., 2004). Instrumental drift was corrected using linear interpolative fits. The U-Pb data (Tables DR1 and DR2) were plotted on a Wetherill Concordia diagram using the software Isoplot (Ludwig, 2001). Uncertainties in these tables were propagated assuming a 1% uncertainty on the age of the standards. ^{204}Pb-based common Pb corrections were not applied because of Hg contamination of the carrier gases.

The analytical runs involved repeated analysis cycles of the GJ-1 standard (ID-TIMS age = 608.5±0.4 Ma; Jackson *et al.,* 2004), NIST-612 glass (Pearce et al., 1997) and Plešovice secondary standard (ID-TIMS age = 337.33±0.38 Ma; Slama *et al.,* 2008), followed by 6-8 unknowns. Laser ablations were performed at a frequency of 10 Hz and an energy density of ~8-8.5 J/cm^2, and produced 30 μm diameter pits. Integration times for U/Pb age determinations were 15 ms for ^{206}Pb, 40 ms for ^{207}Pb, and 10 ms for ^{29}Si, ^{208}Pb, ^{204}Pb, ^{232}Th and ^{238}U. LA-ICP-MS acquisitions consisted of a 20 second measurement of the gas blank, followed by 50 seconds of measurement of Si, U, Th and Pb signals during ablation. U and Th concentrations were extracted from the same integration windows as used for age determinations, using NIST-612 as the external standard and stoichiometric SiO_2 as the internal standard. Twelve analyses of the Plešovice zircon yielded a Concordia age of 339.0 ± 2.8 Ma (95% confidence level (c.l.); MSWD of concordance and equivalence = 1.3), within error of the accepted ID-TIMS age (Slama *et al.,* 2008).

Monazite from the leucocratic garnet-muscovite Salem granite sample N17 was separated from the bulk rock using similar methods to zircon. Monazite was dated at the Research School of Earth Sciences (The Australian National University, Canberra, Australia) using a Resonetics excimer (193 nm) laser coupled to an Agillent 7700 quadrupole ICP-MS. Sixteen micron diameter pits were excavated for each analysis using a laser repetition rate of 5 Hz and an energy of ~ 50 mJ. Data reduction used Glitter software, as described above, and USGS monazite 44069 (424.9±0.4 Ma, Aleinikoff et al., 2006) as the primary standard. Dwell times used were as follows: 10 ms (^{29}Si, ^{88}Sr, ^{89}Y, ^{139}La, ^{140}Ce, ^{141}Pr, ^{146}Nd, ^{147}Sm, ^{151}Eu, ^{157}Gd, ^{159}Tb, ^{163}Dy, ^{165}Ho, ^{166}Er, ^{169}Tm, ^{174}Yb, ^{175}Lu), 20ms (^{31}P) 40ms (^{206}Pb, ^{207}Pb, $^{208}P^{b,}$ ^{232}Th, ^{238}U), with a total ablation time of 40s for each analysis and a 25s blank. Th and U contents were calculated using NIST-610 glass (Pearce et al., 1997) as the external standard and assuming stoichiometric Ce in the monazite.

U/Pb data and sample description

The term Salem-type granite describes a suite of texturally and compositionally distinct, biotite- and/or hornblende- bearing, typically K-feldspar megacrystic granites (Jacob, 1974) than intrude throughout the Damara, from the Southern Zone inland to the Congo Craton. We sampled three Salem-type granites along an approximately N-S transect. Sample localities are given in Figure 1 of main text and a petrographic description is given below.

All sampled plutons show a magmatic foliation defined by the preferred orientation of feldspar megacrysts, elongated wall-rock xenoliths of the Kuiseb Formation and

magmatic enclaves parallel to the margins of the pluton. High-T solid-state foliations are defined by the grain-shape preferred orientation of biotite and quartz ribbons. The solid-state foliation is most pronounced along the margins of the pluton, giving rise to gneissic textures, whereas magmatic foliations dominate the interior of the pluton. Magmatic and solid-state foliations in the pluton show north-easterly strikes parallel to the foliation in the enveloping metaturbidites, but commonly steeper dips to the northwest.

Salem Granite N13, south Central Zone, Damara Belt (23˚ 03.06' S, 14˚ 59.09' E)

Sample N13 was taken close to the Okahandja Lineament Zone, i.e. the southern boundary of the Central Zone, along the C14 road between Walvis Bay and the entrance to the Namib-Naukluft National Park. The sample comes from a mafic megacrystic variant of the Salem Granites and contains quartz, plagioclase feldspar, potassium feldspar, biotite, titanite, zircon and apatite.

Zircon from this sample occurs as prismatic grains 100-175 μm in length. Grains are characterised in CL images by fine, CL-dark euhedral oscillatory zoning, that mantles CL-brighter, more broadly zoned magmatic centres, or broad planar banding. Some oscilltory-zoned grains contain irregular, xenocrystal cores; these are commonly, but not always brighter in CL response than the mantles. Twenty-seven LA-ICP-MS U/Pb analyses were obtained from N13. Five analyses came from xenocrystal cores and yielded weakly (88%) to strongly (38%) discordant analyses with $^{207}Pb/^{206}Pb$ apparent spot ages between c. 1885 Ma and c. 826 Ma (Table DR1; Figure DR1a). Excluding one slightly (94%) discordant analysis with an apparent $^{207}Pb/^{206}Pb$ apparent spot age of 649 Ma (N13-13; Table DR1) twenty one of the remaining 22 analyses of magmatic zircon showed a wide range of Th/U (0.17-1.66) but statistically formed a single population with a Concordia age of 547.5 ± 5.3 Ma (95% confidence level, or c.l.; MSWD of concordance and equivalence = 1.5; Figure DR1b). This is taken to be the best estimate of the emplacement age of the granite.

Salem Granite N15 Southern Zone, Damara Belt (23˚ 33.53' S, 15˚ 02.66' E)

Granite sample N15 is a grey, biotite-rich, megacrystic variant of the Salem granites; it has a similar appearance and mineral assemblage to sample N13. It was sampled in the Namib-Naukluft National Park, near the Gobabeb Training and Research Station.
Zircon grains from this sample are euhedral and prismatic, and 100-175 μm in length. They typically show oscillatory zoning or broad banding of magmatic origin. Inherited cores were rare. Twenty LA-ICP-MS U/Pb analyses are given in Table DR2. Two of the analyses come from inherited cores, are relatively U-rich but concordant, and yield apparent $^{207}Pb/^{206}Pb$ spot ages of c.728 Ma and c. 1009 Ma, respectively. The remainder of the analyses has lower U concentrations (95-396 ppm) and Th/U in the range 0.21-0.90. They form a single population with a Concordia age of 544.0 ± 4.5 Ma (95% c.l., MSWD of concordance and equivalence = 1.5; Figures DR1c and d). This is taken to be the best estimate of the emplacement age of the granite.

Salem Granite N17 Southern Zone, Damara Belt (23˚ 31.78' S, 15˚ 01.45' E)

Granite sample N17 is a pink, medium-grained, non-porphyritic leucocratic granite that contains quartz, plagiolcase feldspar, biotite, muscovite, garnet, zircon, monazite and apatite. It was sampled in the Namib-Naukluft National Park, near the Gobabeb Training and Research Station.

Monazite from this sample occurs as rounded, commonly fractured, an- to subhedral rounded grains, 40-80 μm in diameter, that show weak irregular zoning in BSE images. Sixteen LA-ICP-MS monazite analyses have the same isotopic compositions within uncertainty and yield a concordia age of 543.9 ± 2.9 Ma (2σ; MSWD of concordance and equivalence = 1.0; Figure DR2). Four analyses are displaced away from the Concordia, suggesting the presence of minor common Pb. If these analyses are included an intercept age of 543.5±3.1 Ma (MSWD = 0.46) is obtained. Either age is within error of the zircon LA-ICP-MS U/Pb ages obtained from the mafic megacrystic Salem Granite samples N13 and N15 in this study, and those from the recent literature in the southern Central Zone (Johnson et al., 2009; Kisters et al., 2012). The Concordia age is taken to be the best estimate of the emplacement age of the granite.

Monazite from the Steenkampskraal monazite deposit (Namaqualand, South Africa) was run as a monitor of the accuracy of the monazite U/Pb session. Although not an internationally distributed reference material, it has unpublished SHRIMP weighted mean $^{207}Pb/^{206}Pb$ ages of ca. 1.045 Ga Ma (Buick unpublished data; Knoper, 2010). Nine LA-ICP-MS U/Pb analyses of Steenkampskraal monazite from the same analytical session as N17 yielded a Concordia age of 1034.7 ± 6.3 Ma (MSWD of concordance and equivalence = 1.5; weighted mean $^{207}Pb/^{206}Pb$ age = 1034 ± 15 Ma, MSWD = 0.36), in agreement with the unpublished SHRIMP ages.

References not cited in main text

Aleinikoff, J.N., Schenk, W.S., Plank, M.O., Srogi, LA, Fanning, C. M., Kamo, S. L. and Bosbyshell, H., 2006, Deciphering igneous and metamorphic events in high-grade rocks of the Wilmington Complex, Delaware: Morphology, cathodoluminescence and backscattered electron zoning, and SHRIMP U-Pb geochronology of zircon and monazite: Geological Society of America Bulletin, v.118, p. 39-64.

Frei, D., and Gerdes, A., 2009, Accurate and precise in-situ zircon U-Pb age dating with high spatial resolution and high sample throughput by automated LA-SF-ICP-MS.: Chemical Geology, v. 261, p. 261-270.

Horstwood, M.S.A., Foster, G.L., Parrish, R.R., Noble, S.R. and Nowell, G.M, 2003, Common-Pb corrected in situ U–Pb accessory mineral geochronology by LA-MC-ICP-MS: Journal of Analytical Atomic Spectrometry, v.18, p. 837–846.

Jackson, S. E., Pearson, N.J., Griffin, W. L. and Belousova, E. A., 2004, The application of laser ablation-inductively coupled plasma-mass spectrometry to in situ U-Pb zircon geochronology: Chemical Geology, v. 211, p. 47–69.

Johnson, S.D., Poujol, M. and Kisters, A.F.M., 2006, Constraining the timing and migration of collisional tectonics in the Damara Belt, Namibia: U–Pb zircon ages for the syntectonic Salem-type Stinkbank granite: South African Journal of Geology 109, p. 611–624.

Kisters, A.F.M., Vietze, M.E. and Buick, I.S., 2012, Deformation and age of the Stinkbank pluton and implications for the correlation of tectonometamorphic episodes in the Pan-African Damara Belt: South African Journal of Geology, v. 115, p. 309-326.

Knoper, M.W., 2010, The Mesoproterozoic Steenkampskraal Rare Earth Element deposit in Namaqualand, South Africa: Geological Society of America Abstracts With Programs, v.42, p.335.

Lana, C., Buick, I.S., Stevens, G., Rossouw, R. and De Wet, W., 2011, Upper crustal fold-and-trust tectonics and associated mid-crustal extensional magmatism in the eastern margins of the Barberton Greenstone Belt, South Africa, Journal of Structural Geology, v. 33, p. 844-858.

Ludwig, K.R., 2001, Isoplot/Ex, a geochronological toolkit for Microsoft Excel: Special Publication, Berkeley Geochronological Center, Berkeley, California, v. 1a, pp. 43.

Pearce, N.J.G., Perkins, W.T., Westgate, J.A., Gorton, M.P., Jackson, S.E., Neal, C.R. and Chenery, S.P., 1997, A compilation of new and published major and trace element data for NIST SRM 610 and NIST SRM 612 glass reference materials: Geostandards Newsletter, v. 21, p.115-144.

Sláma, J. Košler, J., Condon, D. J., Crowley, J. L., Gerdes, A., Hanchar, J. M., Horstwood, M. S. A., Morris, G. A., Nasdala, L., Norberg, N., Schaltegger, U., Schoene, B., Tubrett, M. N., and Whitehouse, M. J., 2008, Plešovice zircon – a new natural reference material for U-Pb and Hf isotopic microanalysis: Chemical Geology, v. 249, p. 1–35.

van Achterbergh, E., Ryan, C.G., Jackson, S.E. and Griffin, W., 2001. Data reduction software for LA-ICP-MS, In: P. Sylvester (Editor), Data reduction software for LA-ICP-MS, Laser ablation-ICPMS in the Earth Sciences, Mineralogical Association of Canada, v. 29, p. 239-243.

Supplementary Tables

Table DR1: Zircon LA-ICP-MS U/Pb data from sample N13 and N15.
Table DR2: Monazite LA-ICP-MS U/Pb data from sample N17.

Supplementary Figures

Figure DR1: Concordia diagrams for zircon LA-ICP-MS U/Pb data from sample N13 (a, b) and N15 (c, d).
Figure DR2: Concordia diagrams for monazite LA-ICP-MS U/Pb data from sample N17.

Table DR1: Zircon LA-ICP-MS U/Pb data

Analysis nos	Th (ppm)	U (ppm)	Th/U	$^{207}Pb/^{206}Pb$	1σ	$^{206}Pb/^{238}U$	1σ	$^{207}Pb/^{235}U$	1σ	$^{208}Pb/^{232}Th$	1σ	ρ	Apparent spot ages (Ma) $^{207}Pb/^{206}Pb$	1σ	$^{206}Pb/^{238}U$	1σ	$^{207}Pb/^{235}U$	1σ	$^{208}Pb/^{232}Th$	1σ	% Conc.
N13 Zircon																					
N13-1	168	102	1,66	0,05864	0,0014	0,08892	0,00158	0,7191	0,01829	0,02452	0,00068	0,70	554	51	549,1	9,4	550	11	490	14	100
N13-2	254	753	0,34	0,05714	0,00117	0,08599	0,0017	0,67708	0,01682	0,02335	0,00102	0,80	497	44	532	10	525	10	467	20	101
N13-3	182	354	0,52	0,06088	0,00137	0,08722	0,00183	0,73178	0,01965	0,02229	0,00084	0,78	635	48	539	11	558	12	446	17	97
N13-4	185	240	0,77	0,0596	0,00107	0,08985	0,00151	0,73833	0,01539	0,02584	0,00075	0,81	589	38	554,7	8,9	561,4	9,0	516	15	99
N13-5	137	105	1,30	0,09324	0,0016	0,09167	0,00169	1,17857	0,0249	0,03316	0,00072	0,87	1493	32	565	10	791	12	660	14	38
N13-6	143	102	1,40	0,05878	0,00134	0,08767	0,0017	0,71059	0,01843	0,02814	0,00074	0,75	559	49	542	10	545	11	561	14	99
N13-7	208	162	1,29	0,05918	0,00104	0,0891	0,00152	0,72709	0,01521	0,02821	0,00069	0,82	574	38	550,2	9,0	554,8	8,9	562	14	99
N13-8	432	654	0,66	0,05788	0,00108	0,08597	0,00169	0,68593	0,01619	0,02246	0,00089	0,83	525	41	532	10	530,4	9,8	449	18	100
N13-9	119	163	0,73	0,06109	0,00145	0,08057	0,00159	0,67861	0,01801	0,03065	0,00105	0,74	642	50	499,5	9,5	526	11	610	21	95
N13-10	50	97	0,52	0,11535	0,00233	0,23761	0,00456	3,77834	0,08694	0,08902	0,00449	0,83	1885	36	1374	24	1588	18	1724	83	73
N13-11	148	785	0,19	0,06013	0,00082	0,08777	0,00165	0,72772	0,01463	0,02513	0,00076	0,94	608	29	542,4	9,8	555,2	8,6	502	15	98
N13-12	305	769	0,40	0,06664	0,00099	0,07494	0,00144	0,68843	0,01446	0,01771	0,00058	0,91	826	31	465,8	8,7	531,9	8,7	355	12	88
N13-13	399	832	0,48	0,06127	0,00087	0,07885	0,00147	0,66612	0,01341	0,0271	0,00081	0,93	649	30	489,3	8,8	518,4	8,2	541	16	94
N13-14	453	545	0,83	0,05937	0,0011	0,08545	0,00168	0,69932	0,01636	0,02499	0,00105	0,84	581	40	529	10	538,4	9,8	499	21	98
N13-15	262	234	1,12	0,0589	0,00104	0,08614	0,00164	0,69949	0,0157	0,02566	0,00075	0,85	563	38	532,7	9,8	538,5	9,4	512	15	99
N13-16	179	138	1,30	0,05868	0,00127	0,08836	0,00167	0,71495	0,0177	0,02663	0,00087	0,76	555	46	545,9	9,9	548	10	531	17	100
N13-17	80	151	0,53	0,07381	0,00155	0,15444	0,00301	1,57173	0,03845	0,04873	0,00223	0,80	1036	42	926	17	959	15	962	43	89
N13-18	236	233	1,01	0,05906	0,0009	0,0884	0,00159	0,71982	0,01461	0,02584	0,00065	0,89	569	33	546,1	9,4	550,6	8,6	516	13	99
N13-19	101	602	0,17	0,0602	0,00085	0,08078	0,00143	0,67048	0,01299	0,02836	0,00092	0,91	611	30	500,8	8,5	521,0	7,9	565	18	96
N13-20	158	156	1,01	0,05806	0,00119	0,08789	0,00174	0,70347	0,01737	0,02595	0,00087	0,80	532	45	543	10	541	10	518	17	100
N13-21	135	111	1,22	0,05907	0,00144	0,09011	0,00186	0,73388	0,02036	0,02608	0,00096	0,74	570	52	556	11	559	12	520	19	100
N13-22	186	218	0,85	0,05769	0,00107	0,08933	0,00176	0,71038	0,01666	0,02697	0,00092	0,84	518	40	552	10	545	9,9	538	18	101
N13-23	151	651	0,23	0,059	0,00131	0,09151	0,00205	0,74403	0,02053	0,02378	0,00156	0,81	567	48	565	12	565	12	475	31	100
N13-24	130	123	1,05	0,05817	0,00111	0,08905	0,00169	0,71411	0,01668	0,02567	0,00077	0,81	536	42	550	10	547,2	9,9	512	15	100
N13-25	181	236	0,77	0,05971	0,00093	0,08891	0,00166	0,73193	0,01536	0,02637	0,00081	0,89	593	33	549,1	9,8	557,7	9,0	526	16	98
N13-26	446	388	1,15	0,06687	0,00147	0,06345	0,00133	0,58478	0,01535	0,02415	0,00131	0,80	834	45	396,5	8,0	467,5	9,8	482	26	85
N13-27	269	382	0,70	0,05959	0,00142	0,08965	0,00186	0,73622	0,02015	0,02927	0,00197	0,76	589	51	554	11	560	12	583	39	99
N15 zircon																					
N15_1	74	95	0,77	0,05925	0,00166	0,08889	0,00142	0,72612	0,01991	0,02553	0,00108	0,58	576	60	549,0	8,4	554	12	510	21	99
N15_2	172	661	0,26	0,06358	0,00099	0,11277	0,00151	0,98849	0,01644	0,0355	0,00146	0,81	728	33	688,8	8,7	697,9	8,4	705	29	99
N15_3	87	235	0,37	0,05817	0,00106	0,08723	0,00114	0,69964	0,01287	0,02688	0,00108	0,71	536	40	539,1	6,8	538,6	7,7	536	21	100
N15_4	59	114	0,52	0,05941	0,00174	0,0897	0,00146	0,73462	0,02089	0,02566	0,00153	0,57	582	62	553,7	8,6	559	12	512	30	99
N15_5	103	244	0,42	0,05746	0,00162	0,08691	0,00147	0,68869	0,01937	0,02713	0,00164	0,60	509	61	537,2	8,7	532	12	541	32	101
N15_6	133	148	0,90	0,06017	0,00146	0,08652	0,00133	0,71782	0,01736	0,02752	0,00111	0,64	610	52	534,9	7,9	549	10	549	22	97
N15_7	84	196	0,43	0,06017	0,00132	0,0878	0,00129	0,72839	0,01607	0,02846	0,0013	0,67	610	47	542,5	7,6	555,6	9,4	567	26	98
N15_8	122	489	0,25	0,0586	0,00113	0,08947	0,00132	0,72294	0,01463	0,02854	0,00151	0,73	552	42	552,4	7,8	552,4	8,6	569	30	100
N15_9	37	98	0,38	0,05869	0,00162	0,08731	0,00132	0,70648	0,01876	0,02766	0,00145	0,57	556	59	539,6	7,8	543	11	552	29	99
N15_10	77	117	0,66	0,05933	0,00125	0,08581	0,00121	0,7019	0,01478	0,02591	0,00097	0,67	579	45	530,7	7,2	539,9	8,8	517	19	98
N15_11	93	296	0,31	0,06084	0,0015	0,08581	0,00134	0,7199	0,01772	0,02431	0,0016	0,63	634	52	530,7	7,9	551	10	485	32	96
N15_12	69	148	0,47	0,05764	0,00129	0,08936	0,00131	0,71017	0,01592	0,02637	0,00125	0,65	516	49	551,8	7,7	544,8	9,5	526	25	101
N15_13	70	156	0,45	0,05863	0,00175	0,08749	0,00137	0,70727	0,02019	0,02626	0,00186	0,55	554	64	540,7	8,2	543	12	524	37	100
N15_14	130	203	0,64	0,05935	0,00154	0,09015	0,00141	0,73791	0,01886	0,0267	0,00167	0,61	580	55	556,4	8,3	561	11	533	33	99
N15_15	117	199	0,59	0,06032	0,00138	0,08602	0,00126	0,71545	0,01625	0,02593	0,00152	0,64	615	49	531,9	7,5	548,0	9,6	518	30	97
N15_16	77	215	0,36	0,061	0,00123	0,08955	0,00126	0,75316	0,01539	0,02871	0,00158	0,69	639	43	552,9	7,5	570,1	8,9	572	31	97
N15_17	960	1309	0,73	0,07283	0,00175	0,15955	0,00253	1,60189	0,03855	0,0472	0,00437	0,66	1009	48	954	14	971	15	932	84	98
N15_18	66	133	0,49	0,05834	0,00146	0,08829	0,00129	0,71027	0,01724	0,02696	0,00165	0,60	543	54	545,4	7,6	545	10	538	32	100
N15_19	62	86	0,72	0,05954	0,00179	0,0899	0,00144	0,73804	0,0213	0,02539	0,00165	0,56	587	64	554,9	8,5	561	12	507	32	99
N15_20	81	396	0,21	0,0598	0,00113	0,08679	0,00117	0,71568	0,01358	0,02733	0,00164	0,71	597	40	536,5	6,9	548,1	8,0	545	32	98

% Concordance based on agreement between $^{206}Pb/^{238}U$ and $^{207}Pb/^{235}U$ ages for apparent $^{207}Pb/^{206}Pb$ ages <1.2 Ga; based on agreement between $^{207}Pb/^{206}Pb$ and $^{206}Pb/^{238}U$ ages otherwise
Isotopic data uncorrected for common Pb

Table DR2: Monazite LA-iCP-MS data, N17

	Th	U											Apparent spot ages (Ma)								
Analysis_#	(ppm)	(ppm)	Th/U	$^{207}Pb/^{206}Pb$	1σ	$^{206}Pb/^{238}U$	1σ	$^{207}Pb/^{235}U$	1σ	$^{208}Pb/^{232}Th$	1σ	ρ	$^{207}Pb/^{206}Pb$	1σ	$^{206}Pb/^{238}U$	1σ	$^{207}Pb/^{235}U$	1σ	$^{208}Pb/^{232}Th$	1σ	%Conc.
N17-1	68721	2062	33	0,05874	0,00077	0,08608	0,00103	0,69687	0,01	0,02598	0,00027	0,83	557	28	532,3	6,1	536,9	6,0	518,4	5,4	99
N17-2	89816	3427	26	0,05816	0,00062	0,08754	0,00101	0,70191	0,008	0,0265	0,00027	0,96	535	24	541,0	6,0	539,9	5,0	528,7	5,3	100
N17-3	62526	1061	59	0,05893	0,00089	0,0876	0,00099	0,7117	0,011	0,02689	0,00027	0,73	565	32	541,3	5,9	545,8	6,5	536,4	5,3	99
N17-4	67972	1301	52	0,05991	0,00076	0,08806	0,001	0,72746	0,01	0,02691	0,00027	0,85	600	27	544,0	5,9	555,1	5,7	536,7	5,3	98
N17-5	91532	2189	42	0,06481	0,00085	0,0875	0,00099	0,78182	0,011	0,02625	0,00027	0,82	768	27	540,7	5,9	586,5	6,2	523,7	5,2	92
N17-6	54738	866	63	0,06066	0,00098	0,08881	0,00108	0,74247	0,013	0,0265	0,00028	0,72	627	34	548,5	6,4	563,8	7,4	528,6	5,5	97
N17-7	67718	1037	65	0,05848	0,00094	0,08945	0,00109	0,72097	0,012	0,02634	0,00028	0,72	548	35	552,3	6,4	551,2	7,2	525,5	5,4	100
N17-8	74275	1127	66	0,05889	0,00082	0,08763	0,00105	0,71125	0,011	0,02622	0,00027	0,79	563	30	541,5	6,3	545,5	6,4	523,2	5,4	99
N17-9	72104	1223	59	0,05877	0,00068	0,08838	0,00102	0,71614	0,009	0,02675	0,00028	0,90	559	25	546,0	6,0	548,4	5,4	533,5	5,4	100
N17-10	70603	1150	61	0,0587	0,00073	0,08779	0,00103	0,7104	0,01	0,02648	0,00028	0,87	556	27	542,4	6,1	545,0	5,7	528,2	5,4	100
N17-11	63454	939,8	68	0,0586	0,00082	0,08798	0,00106	0,71065	0,011	0,0265	0,00028	0,79	552	30	543,6	6,3	545,1	6,4	528,7	5,5	100
N17-12	77584	1279	61	0,0587	0,00081	0,08789	0,00106	0,71104	0,011	0,02666	0,00028	0,80	556	30	543,1	6,3	545,4	6,4	531,8	5,5	100
N17-13	105728	1625	65	0,06657	0,00098	0,08681	0,00099	0,79676	0,012	0,0259	0,00026	0,75	825	31	536,6	5,9	595,0	6,9	516,7	5,2	90
N17-14	63826	1315	49	0,05781	0,00074	0,08783	0,001	0,70007	0,01	0,0268	0,00027	0,83	522	28	542,7	6,0	538,8	5,7	534,6	5,4	101
N17-15	65573	1037	63	0,05891	0,0008	0,08823	0,001	0,71676	0,01	0,02734	0,00028	0,79	564	30	545,1	5,9	548,8	6,1	545,1	5,5	99
N17-16	65640	1572	42	0,05864	0,00075	0,08805	0,00105	0,71159	0,01	0,02662	0,00028	0,85	554	28	544,0	6,2	545,7	6,0	530,9	5,5	100
N17-17	74461	3043	24	0,05833	0,00063	0,08766	0,00101	0,70495	0,009	0,0268	0,00028	0,95	542	24	541,7	6,0	541,7	5,1	534,5	5,5	100
N17-18	67075	1101	61	0,05908	0,00116	0,08839	0,00104	0,71995	0,014	0,02762	0,00028	0,59	570	42	546,0	6,2	550,6	8,4	550,8	5,5	99
N17-19	65647	1168	56	0,06417	0,00076	0,0866	0,00102	0,76615	0,01	0,0259	0,00027	0,90	747	25	535,4	6,0	577,6	5,8	516,8	5,4	93

% Concordance based on agreement between $^{206}Pb/^{238}U$ and $^{207}Pb/^{235}U$ ages

Isotopic data uncorrected for common Pb

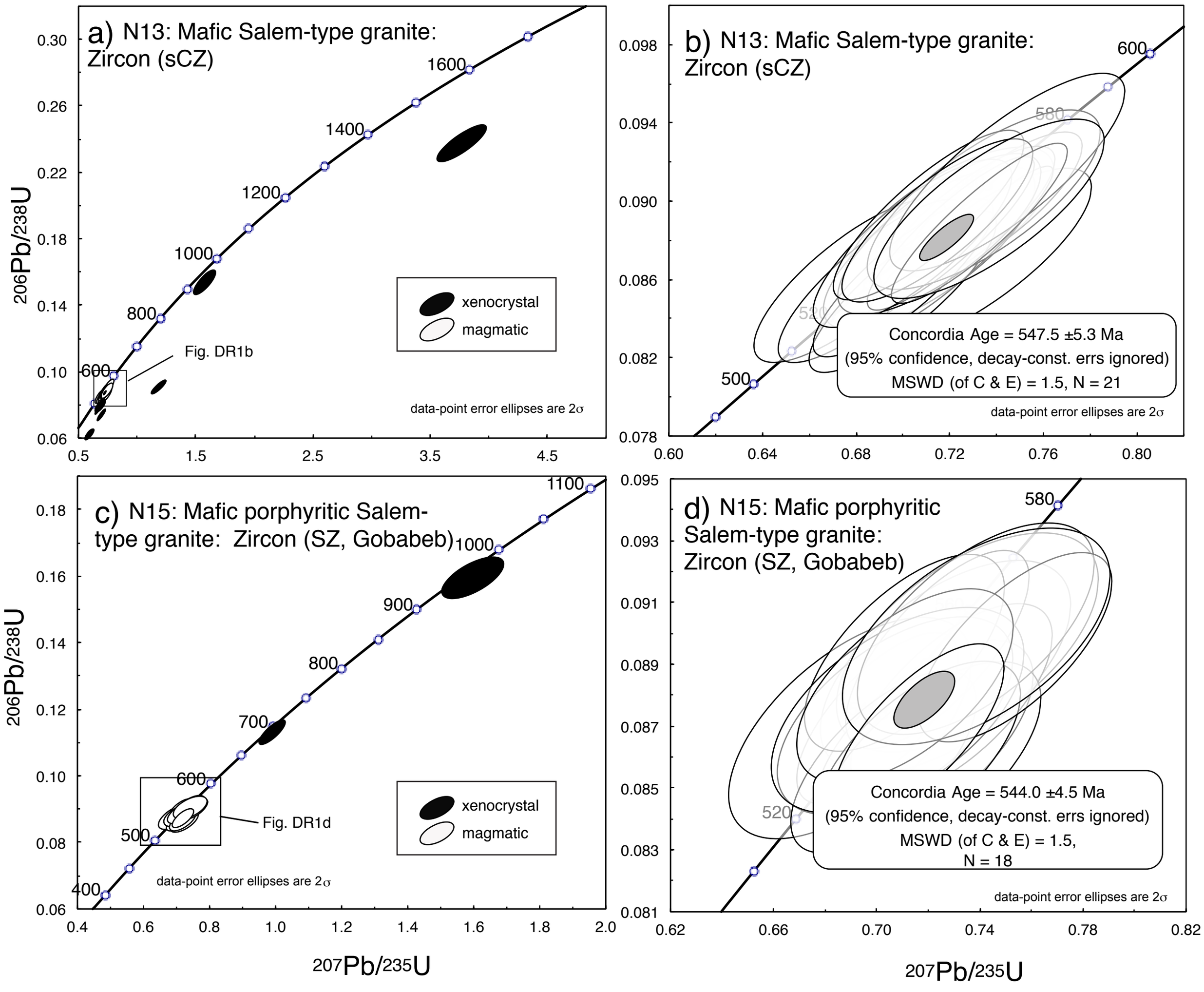

Meneghini et al. Figure DR1

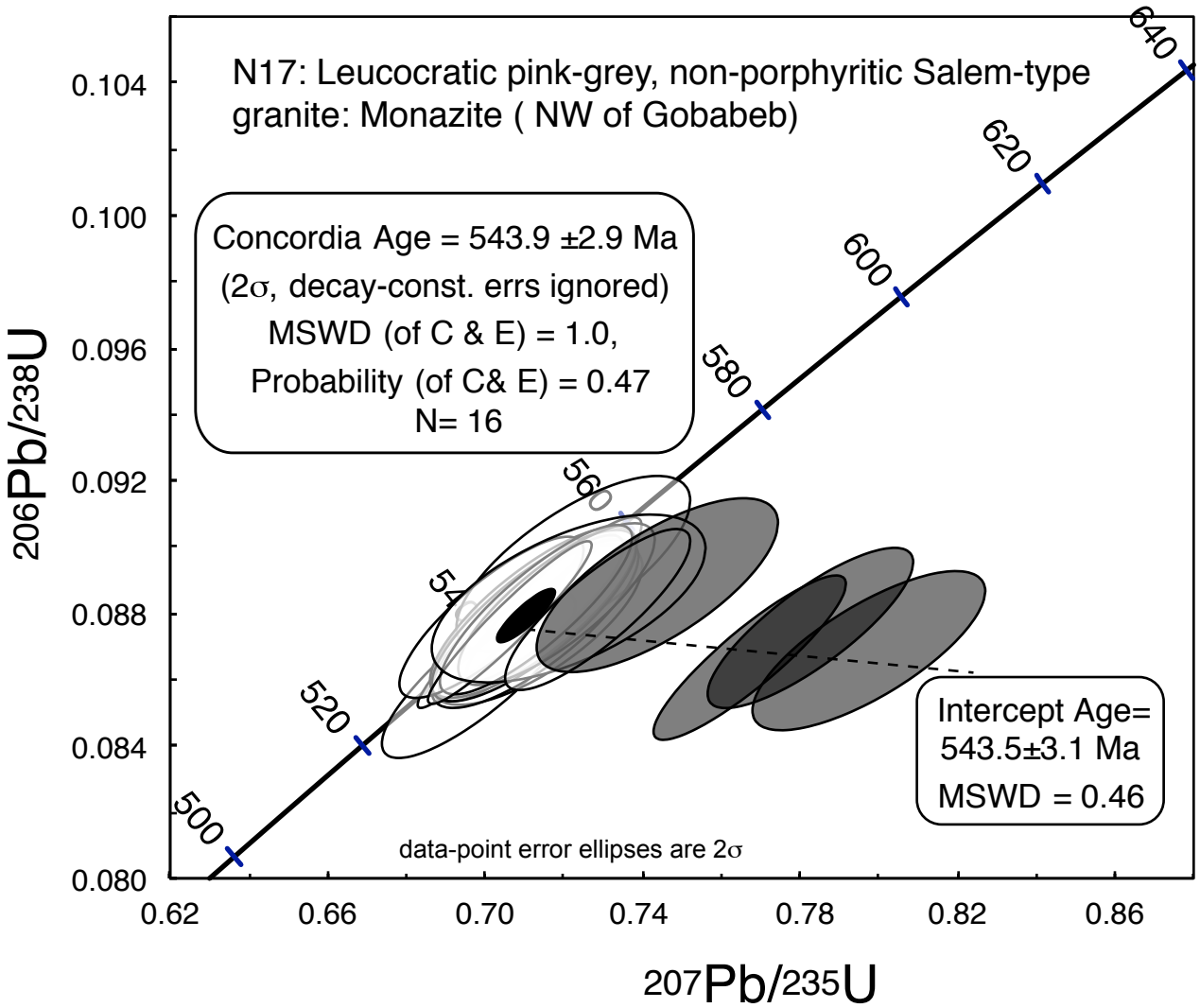

Meneghini et al. Figure DR2